Ninth International Conference on Fast Sea Transportation
FAST2007, Shanghai, China, September 2007

Seakeeping Analysis of the Lifting Body Technology Demonstrator *Sea Flyer* Using Advanced Time-Domain Hydrodynamics

Christopher J. Hart[1], Kenneth M. Weems[2], and Todd J. Peltzer[1]

[1]Navatek, Ltd., Honolulu, Hawaii, USA

[2]Advanced Systems and Technology Division, Science Applications International Corporation, Bowie, Maryland, USA

ABSTRACT

Numerical seakeeping analysis of advanced marine vehicles presents many challenges. Such an analysis was performed for the lifting body technology demonstrator *Sea Flyer*, a 48.8 m converted surface effect ship with a large lifting body amidships and an aft hydrofoil. *Sea Flyer*'s unconventional configuration, the large lift forces generated by the lifting body and aft foil, the transition from floating to flying conditions, and the importance of the dynamic ride control system preclude a traditional linear approach. To address these challenges, we used the Large Amplitude Motions Program (LAMP), a nonlinear, time-domain seakeeping simulation tool based on a 3-D body-nonlinear potential flow solution of the wave-body interaction problem. For the *Sea Flyer* analysis, LAMP's lifting force models were extended and adapted to model the lifting body and a simplified version of *Sea Flyer*'s ride control system was implemented. Seakeeping simulations were performed for a range of sea conditions including those experienced during sea trials and the results show good correlation to the measured sea trials data. This paper presents the characteristics of *Sea Flyer*, a description of the LAMP ship motion calculations, results of the numerical analysis, and a comparison of the predicted motions with sea trials data.

Keywords

Seakeeping, lifting bodies, time-domain simulation.

1 INTRODUCTION

The expanding market for high-speed ships in both the commercial and military sectors in combination with the need to provide accurate performance predictions of such ships in a seaway continues to spur development of innovative hull forms and hydrodynamic analysis tools. There are many challenges in the numerical seakeeping analysis of advanced marine vehicles, among which are the complex geometries and varied operating profiles that are typical of such craft. This is certainly the case for numerical prediction of the motions and loads in waves of the lifting body technology demonstrator *Sea Flyer*, a 48.8 m, 295 t converted surface effect ship (SES) with a large lifting body amidships and an aft hydrofoil. *Sea Flyer*'s unconventional ship configuration, the very large lift forces generated by the lifting body and aft foil, the significant differences in the running waterline as it transitions from floating to flying conditions, and the importance of its installed dynamic ride control system fundamentally preclude the use of traditional linear tools and frequency-domain analysis.

To address these challenges, we used the Large Amplitude Motions Program (LAMP) to conduct the analysis. LAMP is a nonlinear, time-domain ship motion and wave load simulation tool based on a 3-D body-nonlinear potential flow solution of the wave-body interaction problem. LAMP incorporates a wide range of models for viscous and lifting forces not included in potential flow solutions and provides a framework for implementing problem-specific control systems.

This paper presents the characteristics of *Sea Flyer*, a description of the LAMP ship motion calculations, results of the numerical analysis, and a comparison of the predicted motions with sea trials data.

2 *SEA FLYER* CHARACTERISTICS AND SEA TRIALS

Sea Flyer was built principally to demonstrate the scalability, producibility, and hydrodynamic performance benefits of large lifting bodies; a secondary purpose was for use in validating hydrodynamic analysis tools. As noted earlier, it was converted from an SES into a dynamically-supported slender multi-hull vessel, incorporating a patented lifting body (Loui et al. 2006) amidships and a slender horizontal aft foil at the transom (Figure 1, top). The body and foil were each outfitted with a pair of active, hydraulically-actuated trailing edge control surfaces controlled by an advanced ride control system. At 163 t, the lifting body accounts for over half of

the 295 t total displacement and, along with the aft foil, provides enough dynamic lift to fly the hulls clear of the water surface at speeds above 25 knots (Figure 1, bottom). The ride control system provides a smooth transition from hullborne to foilborne modes and the lifting body provides significant motion damping as well. Table 1 provides a summary of *Sea Flyer*'s principal characteristics.

Figure 1 *Sea Flyer* Lifting Body Technology Demonstrator

Table 1 *Sea Flyer* Principal Characteristics

Parameter		Value
Length Overall	160.0 ft	48.8 m
Beam Overall	43.0 ft	13.1 m
Draft, Maximum	18.5 ft	5.6 m
Displacement, Design	290 LT	295 t
Installed Power	2 x 5360 hp	2 x 4000 kW
Speed	30+ knots	

Lifting bodies are underwater appendages with cambered foil cross sections that generate dynamic lift at speed. They are characterized by substantial volume, large planform areas, and low lift coefficients. Figure 2 shows the *Sea Flyer* lifting body while in dry dock during installation (the view is looking aft). A detailed discussion of the benefits of lifting bodies and their application in a number of technology demonstrators is provided by Peltzer (2007).

Sea Flyer's advanced ride control system provides ride enhancement while hullborne and complete dynamic flight control and maneuvering, including coordinated turns, while foilborne. The system architecture employs redundant critical sensors (dual height sensors at the bow and dual inertial motion reference units) and triple digital control computers operating in parallel using a 'voter' scheme to drive the hydraulic servo-valves at each control surface. This arrangement allows for graceful degradation of system performance in the event of component failure.

Figure 2 *Sea Flyer* in Dry Dock Showing Lifting Body

Sea Flyer has undergone extensive instrumented sea trials in Hawaiian waters to characterize its performance and a significant volume of data has been recorded and documented (Hill et al. 2005). These trials included speed/power and fuel economy testing at three displacements (274 t, 295 t, and 325 t) and three flying heights (at 274 t displacement); acceleration and deceleration testing; turning circles and horizontal overshoot; and seakeeping trials in two sea states (SS3 and SS4). Additional testing and extensive operation of *Sea Flyer* in up to 3.5 m seas demonstrated her exceptional performance, especially her ride quality.

In support of future lifting body ship design efforts we were interested in developing seakeeping analysis tools that would allow us to accurately predict the performance of configurations such as *Sea Flyer*. Based on previous experience in using LAMP for analysis of lifting body ships at zero and low speed, a collaborative effort to enhance its ability to model dynamically supported vehicles with closed-loop control systems was undertaken, resulting in an extended version of LAMP that was then validated against the data from the *Sea Flyer* seakeeping trials.

The following sections describe the computational methodology used in LAMP, the modeling of *Sea Flyer* in LAMP, and a comparison of LAMP results with sea trials data.

3 LAMP COMPUTATIONAL METHODOLOGY

LAMP is a nonlinear time-domain potential flow seakeeping code developed to predict the motions and loads of a ship or other marine vehicle in a seaway. LAMP development began in 1988 to supplement traditional frequency-domain methods in the prediction of nonlinear hull loads of large naval combatants and commercial ships in severe sea conditions. Since then, LAMP's time-domain approach, 3-D geometry model, nonlinear hydrodynamics, and flexible external force and system models have allowed it to be used for the analysis of a wide variety of conventional and unconventional ships and marine vehicles including tumblehome and multi-hull ships, high-speed displacement hulls, buoys,

and offshore platforms (Shin et al. 2003). These features have also allowed LAMP to be used for the analysis of a number of novel ship configurations such as *Sea Flyer* that incorporate large lifting bodies or blended wing-body appendages.

Key features of the LAMP computational methodology include:

- Time-stepping approach in which all forces and moments acting on the ship are computed at each time step.
- Solution of the wave-body hydrodynamic interaction problem with forward speed using a 3-D potential flow panel method.
- Time-domain integration of the six-degree-of-freedom equations of motion using a 4th-order Runge-Kutta algorithm.
- Main girder load calculation using a rigid or elastic beam model and an interface for developing finite-element load data sets from the 3-D pressure distribution (Weems et al. 1998).
- Models for additional effects and systems including viscous and lifting forces for hull and appendages, course and motion control systems, and green water.

3.1 Wave-Body Hydrodynamics

The core of the LAMP calculation is the 3-D solution of wave-body interaction problem in the time domain. A 3-D perturbation velocity potential is computed by solving an initial boundary value problem using a potential flow boundary element or 'panel' method. A combined body boundary condition is imposed that incorporates the effects of forward speed, the ship motion (radiation), and the scattering of the incident wave (diffraction). Once the velocity potential is computed, Bernoulli's equation is then used to compute the hull pressure distribution including the second-order velocity terms.

The perturbation velocity potential can be solved over either the mean wetted surface (the 'body-linear' solution) or over the instantaneously wetted portion of the hull surface beneath the incident wave (the 'body-nonlinear' approach). In either case, it is assumed that both the radiation and diffraction waves are small compared to the incident wave and the incident wave slope is small so that the free surface boundary conditions can be linearized with respect to the incident wave surface. Similarly, the incident wave forcing (Froude-Krylov) and hydrostatic restoring force can also be computed either on the mean wetted surface or on the wetted hull up to the incident wave.

The combinations of the body-linear and body-nonlinear solutions of the perturbation potential and the hydrostatic/Froude-Krylov forces provide multiple solution 'levels' for the ship-wave interaction problem. These levels are:

- Body-linear solution: Both perturbation potential and Froude-Krylov forces are solved over the mean wetted hull surface; restoring forces are computed from the geometry of the static waterplane.
- Approximate body-nonlinear solution: The perturbation potential is solved over the mean wetted hull surface while the hydrostatic restoring and Froude-Krylov forces are solved over the instantaneous wetted hull surface.
- Body-nonlinear solution: Both the perturbation potential and the hydrostatic/Froude-Krylov forces are solved over the instantaneous wetted hull surface.

For most ship motion and load problems, the 'approximate body-nonlinear' solution has been found to capture the most significant nonlinear effects at a fraction of the computational effort required for the general body-nonlinear formulation. This is the solution used for the *Sea Flyer* analysis.

3.1.1 Potential Flow Singularity Model

Several techniques have been implemented to compute the wave-body disturbance potential. The basic solution involves direct solution of the boundary value problem using one of two singularity models: a hybrid singularity model that uses both transient Green functions and Rankine sources (Lin et al. 1999), or a Rankine singularity model with a numerical damping zone (Kim & Weems 2000).

While the former model provides a more 'complete' treatment to the far-field free surface condition, the latter has proved to be more robust for higher speed runs ($Fr > 0.5$) and has been successfully applied to high-speed displacement hulls ($Fr > 0.85$). The Rankine singularity model also allows finite water depth to be modeled in the wave-body hydrodynamics.

3.1.2 IRF-Based Approach

A drawback to time-domain hydrodynamics is the computational cost. To mitigate this, an impulse response function (IRF) based hydrodynamic formulation (Liapis 1986, King et al. 1988, Bingham et al. 1993) was integrated into the LAMP system to complement the mixed source formulation. In the IRF formulation, velocity potentials are pre-computed for steady forward speed, impulsive motion in up to six modes, and impulsive incident waves for each speed and heading angle. The hydrodynamic problem is thus reduced to a convolution of the IRF potentials with the actual ship motions and incident wave elevation, thereby significantly reducing the computational cost without compromising the accuracy of the hydrodynamic calculation.

The IRF potentials are convoluted and summed on a panel-by-panel basis, so that the complete potential distribution of the hull can be computed in the time domain. This allows the panel pressure to be computed directly, including the nonlinear terms in Bernoulli's equation, in the same fashion as in the mixed-source formulation. The only restriction is that the IRF formulation can only be used with 'body-linear' and 'approximate body-nonlinear' hydrodynamic solutions.

Implementation of the IRF-based approach is described in more detail in Weems et al. 2000 and Shin et al. 2003.

3.2 Supplemental Force Models

While the solution of inviscid wave-body hydrodynamic interaction problems typically captures the most important effects for the simulation of a ship in waves, other effects such as viscous and lifting forces and control systems can be significant for particular problems or configurations (e.g. *Sea Flyer*). To account for these effects, a range of external force and system models have been incorporated into the LAMP code, including:

- Viscous roll damping
- Appendage lift and drag
- Hull lift maneuvering forces
- Course-keeping autopilot
- Green-water-on-deck
- Internal tanks and flooding
- Mooring systems
- Ride control systems
- Tank and fin roll-control systems
- Propulsion systems

These models are implemented in the time domain and compute the forces acting on the ship as a function of the ship motion, incident wave, and other data. They range in complexity from a simple regression-based equation for viscous roll damping to a fully coupled finite-volume flow solution of green-water-on-deck. Many of the models include multiple modeling options, approaches, and/or levels.

For *Sea Flyer*, accurately modeling lift and drag forces acting on the lifting body and other appendages and incorporating the ride control system were essential to producing a reliable seakeeping analysis.

3.2.1 Lift Models

Since viscosity and vorticity are not explicitly included in LAMP's potential flow solution, a series of external force models have been implemented for calculation of the lift, induced drag, and viscous drag of the hull and appendages. The appendage models can be used both for large appendages that are included in the potential flow panel model, such as *Sea Flyer*'s lifting body, and for smaller appendages that are not panelized, such as the rudder in a typical ship calculation.

The lift models include built-in expressions based on the appendage geometry plus an option to enter lift curve data. In the lift calculation, the vector inflow velocity to each appendage is computed by evaluating the relative velocity of an appendage reference point from the ship's rigid body motion plus the orbital velocity of the incident wave field. The geometry of the appendage plus any appendage deflections are used to resolve the velocity into chord-wise, span-wise, and normal components from which an effective inflow velocity, V, and angle of attack, α, can be derived. For long or large appendages, this evaluation can be performed at multiple span-wise locations, primarily in order to account for the variation in inflow velocity vector due to roll velocity.

Basic Lift – The basic lift model, equations (1) through (3), uses the standard expressions for the lift generated by low aspect ratio fully movable foils as presented in *Principles of Naval Architecture* (Comstock ed. 1967) and other standard texts:

$$Lift = C_L \cdot \rho V^2 A_P \tag{1}$$

$$C_L = \frac{\pi}{2} A_R \cdot \alpha : A_R < 2.0, \alpha < \alpha_{stall} \tag{2}$$

$$C_L = \frac{2\pi}{1+\frac{2}{A_R}} \cdot \alpha : A_R \geq 2.0, \alpha < \alpha_{stall} \tag{3}$$

Here ρ is the water density, A_P is the planform area, and A_R is the effective aspect ratio, which can include ground boarding or end plating. These expressions are used up to a specified stall angle, α_{stall}, after which an 'eddy-making' expression is invoked.

Flap Lift – For appendages with full or partial flaps equations (4) through (6), based on von Mises (1945), are used to compute the incremental lift and moment about the foil leading edge:

$$\Delta C_L = 2\delta(\phi + \sin\phi - \lambda\phi) \cdot \Lambda \tag{4}$$

$$\Delta C_M = -\tfrac{1}{2}\delta(\sin\phi + \tfrac{1}{2}\sin 2\phi) \cdot \Lambda \tag{5}$$

$$\phi = \cos^{-1}(1 - 2\lambda) \tag{6}$$

Here λ is the ratio of the flap chord to the foil chord, Λ is the ratio of the flap span to the foil span, and δ is the flap deflection angle.

Lift Effect With Submergence – Foils moving parallel to and near the free surface will experience a loss of lift as they get very close the surface. This loss of lift can be very important for determining the flying height of vessels such as *Sea Flyer*. To account for this, the following expression has been implemented from Faltinsen (2004):

$$C_L = C_L^{deep} \cdot \left[\frac{1 + 16(h/c)^2}{2 + 16(h/c)^2} \right] \tag{7}$$

Here C_L^{deep} is the base 'deep water' lift coefficient, c is the chord length and h is the submergence of the foil beneath the incident wave surface.

Specified Lift Curve Data – For cases where appendage lift characteristics can be calculated or measured externally, lift data curves or tables can be specified. This data includes the appendage's lift, moment about the spanwise vector, and drag relative to a specified reference point and can be specified with respect to the angle of attack, flap deflection angle, and/or submergence beneath the wave surface. For cases where the depth dependence is not explicit, specified deep water lift data can be used with the submergence correction from equation (7).

This option allows high-fidelity lift data computed from lift analysis programs such as XFOIL, viscous flow

solvers such as CFX, or systematic model tests, to be incorporated in the LAMP simulation.

3.2.2 Control System Models

LAMP control system models include a course-keeping autopilot, propulsion controller, several roll-control systems, and a general foil controller for ride and motion control. Some of these controllers, such as the U-tank roll controller, are built into supplemental force models while others, like the course-keeping autopilot, are used to control the deflection of an appendage or a flap on an appendage. For the latter type of controllers, a fairly simple servo model is used to compute the realized fin deflection at each time step while the resulting forces are computed using the procedure described in Section 3.2.1.

The ride and motion controller allows the specification of a target riding height and trim angle and PID (proportional, integral, and differential) gains for deflection due to any of the vertical motion displacements and derivatives. More sophisticated control laws incorporating surrogate wave sensor models and other effects, adaptive neural-network based controllers, and other systems have also been modeled in LAMP for specialized applications.

4 LAMP MODELING OF *SEA FLYER*

4.1 Geometry and Panel Model

The geometry model used in the LAMP hydrodynamic model was developed by creating point definition patches over the CAD surface model (Figure 3).

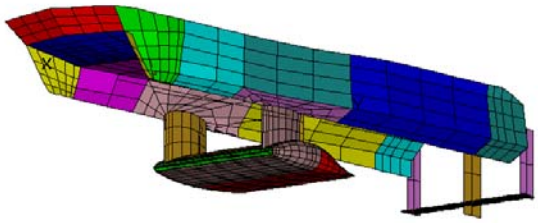

Figure 3 Sea Flyer Geometry Model

For the solution of the wave-body disturbance potential, a 3-D panel model was created by truncating this geometry model at the mean waterline and generating a fitted free surface panel grid both between and outside the hulls. A portion of a typical panel model is shown in Figure 4.

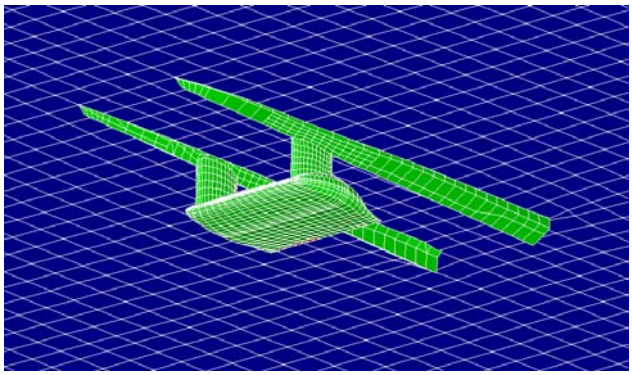

Figure 4 Hull and Local Portion of the Free Surface Panel Grid

As shown here, the lifting body and struts were included the panel model but the aft appendages were not. Test calculations that included the aft cross foil in the potential flow calculation showed negligible contribution to the inviscid hydrodynamic problem, though the lift of these appendages was modeled as described below.

4.2 Hydrodynamic Modeling Options

Most of the LAMP simulations were performed using the approximate body-nonlinear approach in which the disturbance potential is computed over the mean wetted surface while the incident wave forcing and hydrostatic restoring forces are computed over the instantaneous wetted hull surface. This is the approach used for most LAMP analyses as it has been found to capture the most significant nonlinear aspects of the wave-body interaction problem at a very reasonable computational cost.

For *Sea Flyer*, however, there was concern that the large difference between the static flotation and the flying configuration might compromise this approach. To check this, we ran simulations in which the calculation of the disturbance potential was linearized about both the static waterline and several flying heights and trims. Figure 5 compares the mean flying position at 27 knots (top image) with the static waterline (bottom image). These calculations showed very little sensitivity of the predicted motions in waves to the selected hull linearization.

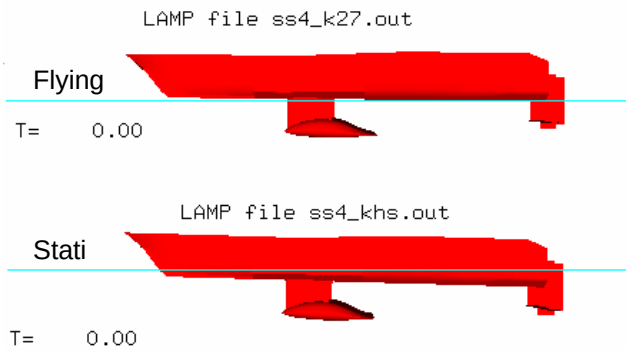

Figure 5 Static and Flying Waterlines for Linearization

As a further check, we made a few test simulations using the body-nonlinear approach, in which the disturbance potential is computed over the time-varying wetted portion of the hull up to the incident wave surface. Comparing these results to the corresponding approximate body-nonlinear calculations showed that the much more expensive body-nonlinear approach was not needed for the *Sea Flyer* analysis.

Due to the relatively high speed of *Sea Flyer* in the faster trials runs, all of the simulations used the Rankine singularity model with damping beach. Because many simulations were required to work out the modeling of the ride control system, the IRF-based hydrodynamic formulation was used.

4.3 Ride control

The ride control system as implemented in LAMP was a reasonable but approximate representation of the *Sea Flyer* system. The lifting body, cross foil with vertical

struts, and the trailing edge control flaps on both the cross foil and lifting body were modeled in LAMP using the simple appendage model (Figure 6).

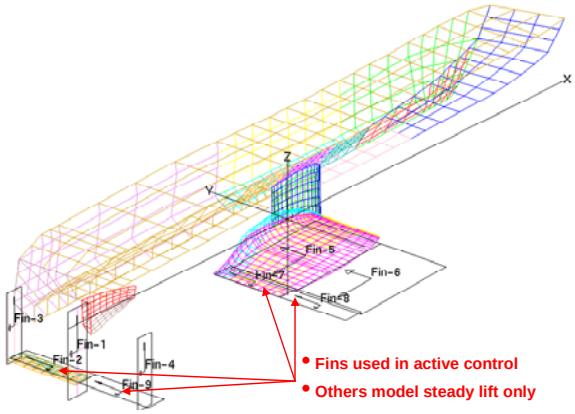

Figure 6 Appendage Model for LAMP Simulations

The incidence angles of the appendages representing the lifting body and aft cross foil were set to provide the proper mean lift at the design flying height and trim. The trailing edge flaps on the lifting body were modeled as a separate pair of control surfaces; the aft foil's control flaps were represented by deflection of each half of the foil to provide control forces. The lifting body flaps contributed both to heave control and roll control, while the aft control surfaces were actuated for roll, pitch, and heave.

A commanded flying height and running trim were set in LAMP's Foil Control module along with characteristics of actuator rate, maximum fin angle, and bandwidth. Initially, simple proportional gains appeared to provide stable flight and reasonable motions but after comparison to measured trials data, the addition of rate gain to the roll control provided better correlation. Interestingly, when comparing the magnitudes and rates of these simplified surfaces to actual *Sea Flyer* data the behavior was remarkably similar.

The starting point for the control system gain settings was based primarily on the proportional components of *Sea Flyer*'s actual gains. However, since the control surfaces and the LAMP PID controller are a simplification of *Sea Flyer*'s actual system, the setup in LAMP involved some trial and error to set and verify the appropriate gains and particularly the polarities. We made several series of calm water runs, perturbing the model and observing the response of the foils to verify the gain settings, polarities, and general stability of the model. One result was that because of the importance of the appendage forces and the control system in balancing the pitch, a shorter than normal time step was required to maintain the stability of LAMP's explicit time-stepping approach.

4.4 Seaway Modeling

There are several methods in LAMP for modeling a seaway including a number of standard sea spectra such as Pierson-Moskowitz, Bretschneider, and JONSWAP. LAMP also has the capability to use wave height time history data to recreate a phase-resolved representation of actual seaway conditions.

For *Sea Flyer*, initial LAMP runs were performed using a Bretschneider two-parameter long-crested (unidirectional) spectrum derived using a nominal characterization of the trials conditions. Additional simulations were made using a short-crested option that distributed the wave energy directionally using a cosine-squared spreading function. These latter runs took longer but provided a more realistic wave field and generally better correlation. During sea trials, which were conducted in the waters south of the island of Oahu, the 20 to 30 minute run times at each heading covered enough distance that the wave patterns and magnitudes changed over the course of a given run. Observations were noted in the trials log about a secondary swell; however, directional wave measurements were not recorded. To account for this in the LAMP simulations, several additional sea states were modeled using significant wave heights and modal periods that corresponded more closely to those experienced during each phase of the trials; however, no attempt was made to simulate separate wave conditions for each individual test run, nor was sufficient data available to attempt a phase-resolved reconstruction. These sets of seaways bounded the observed wave heights and periods encountered during the trials and allowed us to evaluate the sensitivity of the motion responses to sea state. The result of this sensitivity analysis was that while the correlation at any one speed-sea state-heading condition may not match perfectly, the magnitudes and trends in motion response as a function of speed, heading, and sea state tracked remarkably well and built confidence in the LAMP model.

5 RESULTS AND COMPARISON TO TRIALS DATA

Many LAMP simulations of *Sea Flyer* were performed at a variety of running conditions from hullborne to fully flying in sea conditions from calm water to large multidirectional seas, and with variations in ride control settings such as flying height and control gains. During this process, we studied various approaches to modeling the surface geometry, the control surface approach, computational options, degrees of freedom, etc. While some simulations were conducted with six degrees of freedom, most were conducted with surge, yaw, and sway restrained. Although these modes can be modeled in LAMP they are computationally expensive and potentially dependent on the course control modeling, and due to the large number of headings, sea states, and speed combinations being analyzed these modes were left for future analysis.

For the sea trials correlation cases, LAMP simulations were conducted at speeds of 5, 10, 15, and 27 knots. These simulations were run for an equivalent of 6 minutes in real time at each combination of speed, heading, and sea state. Summary statistics for motions and control surface angles were computed and compiled for each simulation series and were plotted against the trials data.

While longer simulations would be required for long term statistics, these were adequate for comparison to trials data.

Figure 7 compares predicted vs. measured motions in sea state 4 (SS4) at 27 knots. The simulations are for a short-crested seaway with a significant wave height and modal period of 2 m and 6.0 seconds, respectively. The upper plot in Figure 7 shows RMS vertical acceleration at the vertical center of gravity in g over a range of headings from 0 to 315 degrees where 0 deg is following seas, 180 deg is head seas, and 90 deg is starboard beam seas. The center and lower plots in Figure 7 similarly show the roll and pitch significant amplitudes (in degrees). As mentioned earlier, the sea conditions changed somewhat over the trials period, so the correlation is not expected to be exact but illustrates that for this fully-flying configuration the trends and magnitudes of motion are being captured with reasonable accuracy.

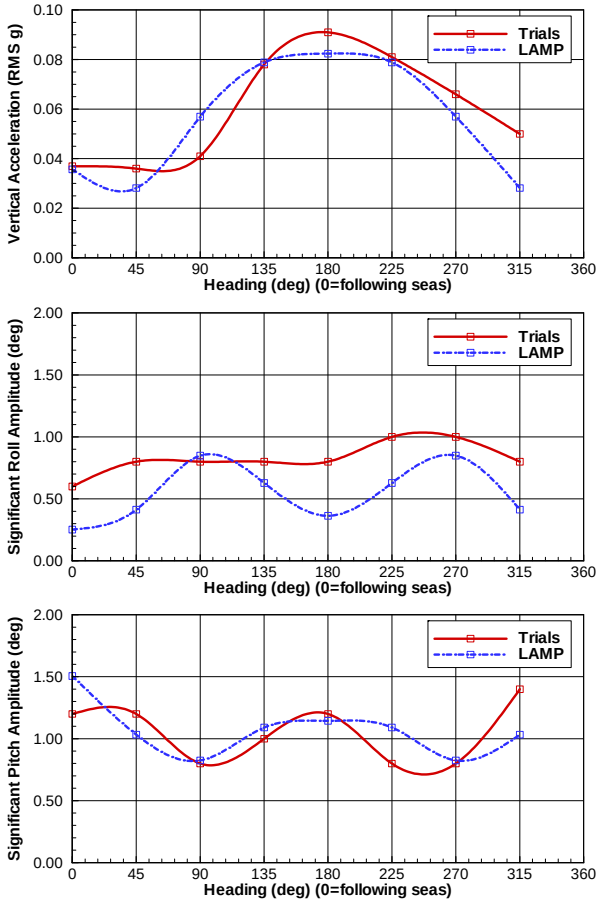

Figure 7 LAMP vs. Trials Data: 27 knots, SS4

The correlation between simulation and sea trials as a function of both speed and sea state is illustrated in Figure 8, which compares the motions at 15 knots for SS3 and SS4. Vertical acceleration (RMS g) is given in the upper plot, and roll and pitch significant amplitudes (in degrees) are given in the center and lower plots, respectively. Note that the magnitudes of the motions are greater than for the 27 knot case; this is due largely to the immersion of the hulls. The conditions at 15 knots correspond to a transition state with *Sea Flyer*'s side hulls still in displacement mode and not yet flying (which occurs at approximately 25 knots), yet the ride control system is contributing significantly to motion stabilization at this speed. During the 15 knot trials the measured SS4 seaway was steeper than for the 27 knot case, with a typical significant wave height and modal period of 2.2 m and 5.8 seconds, respectively. For the 15 knot, SS3 case the significant wave height was 1.1 m with a modal period of 12.5 seconds.

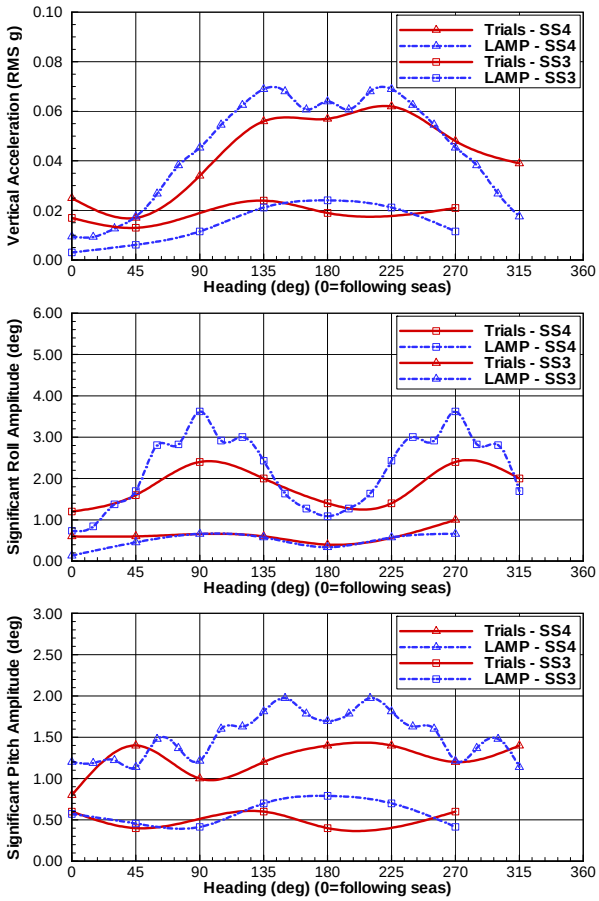

Figure 8 LAMP vs. Trials Data: 15 knots, SS3 & SS4

In addition to the quantitative comparison of motion statistics, 3-D visual animations of the predicted time domain ship motions were used to quickly assess the validity of each simulation run and to spot potential input errors or issues of model stability (Figure 9). Viewing the 3-D animations qualitatively confirmed that the nature of the motions was also very similar to the actual motions observed.

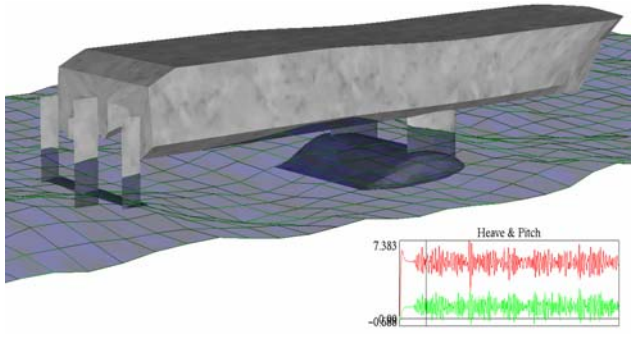

Figure 9 LAMP Animation Frame: 27 knots, SS4

In addition to the motion data, the hull pressure distribution and free surface elevations can be saved and plotted to show how the panel model and flow solution vary as the vessel cycles in waves. Figure 10 shows a snapshot of *Sea Flyer*'s panelization, hull pressure, and disturbance waves in a SS4 bow quartering run. Such pressure distributions can be stored with acceleration data at critical maximum load cases and exported for use in FEA analysis.

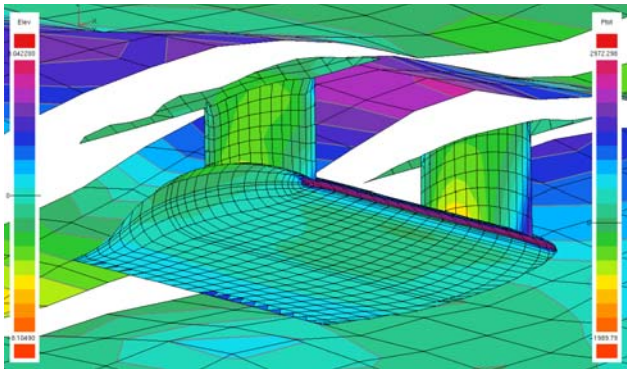

Figure 10 Pressure Distribution and Free Surface Elevation

6 CONCLUSIONS

We successfully demonstrated that LAMP can be used to model the seakeeping behavior of an advanced marine vehicle with a complex geometry and a widely varying operating profile. To do so, LAMP's lifting force models were extended and adapted to model lifting bodies, and new capabilities were added to model movable control surfaces and to model basic PID control systems.

The wealth of data produced during instrumented sea trials of *Sea Flyer* presented an opportunity to partially validate these changes to LAMP. The results showed that LAMP credibly predicts the motions across a broad range of speeds, headings, sea states, and ride control parameters. The experience gained in adapting and applying LAMP to *Sea Flyer*'s unique attributes provides confidence in its use as a tool for application to other advanced vessel concepts.

ACKNOWLEDGEMENTS

Much of the work described in this paper was made possible with support from the Office of Naval Research. The development of the LAMP System has been supported in part by the U.S. Navy, the Defense Advanced Research Projects Agency, the U.S. Coast Guard, and the American Bureau of Shipping.

REFERENCES

Bingham, B., Korsmeyer, F., Newman, J., & Osborne, G. (1993). 'The Simulation of Ship Motions.' Proceedings of the 6th International Conference on Numerical Ship Hydrodynamics, Iowa City, IA, USA, pp. 27–47.

Comstock, J. P. (ed.) (1967). Principles of Naval Architecture. The Society of Naval Architects and Marine Engineers.

Faltinsen, O. M. (2005). Hydrodynamics of High-Speed Marine Vehicles. Cambridge University Press, Cambridge, UK.

Hill, B., Bachman, R., Powell, M., & Woolaver, D. (2005). 'Sea Flyer HYSWAC (Hybrid Small Waterplane Area Craft) Performance and Special Trials Results.' Naval Surface Warfare Center, Carderock Division, NSWCCD-50-TR-2005/053, West Bethesda, MD, USA.

Kim, Y., & Weems, K. M. (2000). 'Motion Responses of High Speed Vessels in Regular and Random Waves.' Proceedings of the Royal Institution of Naval Architects Conference on the Hydrodynamics of High Speed Craft, London, England.

King, B., Beck, R., & Magee, A. (1988). 'Seakeeping Calculations with Forward Speed Using Time Domain Analysis.' Proceedings of the 17th Symposium on Naval Hydrodynamics, The Hague, The Netherlands.

Liapis, S. (1986). 'Time-Domain Analysis of Ship Motions.' Report 302, Department of Naval Architecture and Marine Engineering, University of Michigan.

Lin, W.-M., Zhang, S., Weems, K. M., & Yue, D. K. P. (1999). 'A Mixed Source Formulation for Nonlinear Ship-Motion and Wave-Load Simulations.' Proceedings of the 7th International Conference on Numerical Ship Hydrodynamics, Nantes, France, pp. 1.3.1–12.

Loui, S., Shimozono, G., & Keipper, T. (2006). 'Low Drag Submerged Asymmetric Displacement Lifting Body.' U.S. Patent No. 7,004,093, B2.

Peltzer, T. J., (2007). 'Recent Developments in Lifting Body Ships and Small, High-Speed Hull Forms.' ASNE High Speed High Performance Ships and Craft Symposium 2007, Annapolis, MD, USA.

Shin, Y.-S., Belenky, V. L., Lin, W.-M., Weems, K. M., Belknap, W. F., & Engle, A. H. (2003). 'Nonlinear Time Domain Simulation Technology for Seakeeping and Wave Load Analysis for Modern Ship Design.' Transactions of the Society of Naval Architects and Marine Engineers **111**, pp. 557-578.

von Mises, R. (1945). Theory of Flight. Dover Publication, Toronto, Canada.

Weems, K. M., Zhang, S., Lin, W.-M., Shin, Y.-S, & Bennett, J. (1998). 'Structural Dynamic Loadings Due to Impact and Whipping.' Proceedings 7th International Symposium on Practical Design of Ships and Mobile Units, The Hague, The Netherlands.

Weems, K. M., Lin, W.-M., Zhang, S., & Treakle, T. (2000). 'Time Domain Prediction for Motions and Loads of Ships and Marine Structures in Large Seas Using a Mixed-Singularity Formulation.' Proceedings of the Fourth Osaka Colloquium on Seakeeping Performance of Ships (OC2000), Osaka, Japan, pp. 272-280.